

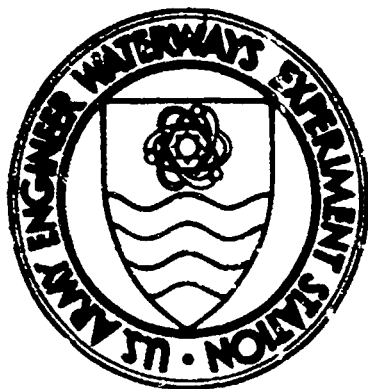
U.S. DEPARTMENT OF COMMERCE
National Technical Information Service

AD-AG32 903

EFFECT OF PRESSURE DISTRIBUTION UNDER PNEUMATIC
TIRES ON STRESSES AND DISPLACEMENTS IN THE
SUPPORTING ELASTIC MEDIA

ARMY ENGINEER WATERWAYS EXPERIMENT STATION,
VICKSBURG, MISSISSIPPI

MAY 1970



MISCELLANEOUS PAPER M-70-6

**EFFECT OF PRESSURE DISTRIBUTION UNDER
PNEUMATIC TIRES ON STRESSES AND
DISPLACEMENTS IN THE SUPPORTING
ELASTIC MEDIA**

by

Y. T. Chou

D R A F T



May 1970

Sponsored by U. S. Army Materiel Command

Project IT061102B52A

Task 01

Conducted by U. S. Army Engineer Waterways Experiment Station, Vicksburg, Mississippi

ARMY-MRC VICKSBURG, MISS.

~~This document is subject to~~

DISTRIBUTION STATEMENT A

**Approved for public release;
Distribution Unlimited**

~~This document is subject to~~

Unclassified

Security Classification

DOCUMENT CONTROL DATA - R & D

(Security classification of title, body of abstract and indexing annotation must be entered when the covered report is classified)

1. ORIGINATING ACTIVITY (Corporate author) U. S. Army Engineer Waterways Experiment Station Vicksburg, Miss.		2a. REPORT SECURITY CLASSIFICATION Unclassified	
3. REPORT TITLE EFFECT OF PRESSURE DISTRIBUTION UNDER PNEUMATIC TIRES ON STRESSES AND DISPLACEMENTS IN THE SUPPORTING ELASTIC MEDIA			
4. DESCRIPTIVE NOTES (Type of report and inclusive dates) Final report			
5. AUTHOR(S) (Last name, middle initial, first name) Yu-Tang Chou			
6. REPORT DATE May 1970	7a. TOTAL NO. OF PAGES 37	7b. NO. OF REFS 8	
8a. CONTRACT OR GRANT NO. a. PROJECT NO. 1T061102B52A c. Task 01 d.		8b. ORIGINATOR'S REPORT NUMBER(S) Miscellaneous Paper M-70-6	
8c. OTHER REPORT NUM(S) (Any other numbers that may be assigned this report)			
9. DISTRIBUTION STATEMENT			

DISTRIBUTION STATEMENT A
 Approved for public release;
 Distribution Unlimited

U. S. Army Materiel Command
 Washington, D. C.

10. ABSTRACT

square meters

The validity of the assumption of uniform pressure distribution under a pneumatic tire was checked in this study. Measurements of pressure distributions under pneumatic tires at their interface with firm surfaces and soft soils, previously made at the U. S. Army Engineer Waterways Experiment Station, were used. Two tires (11.00-20, 12-PR, and 12-22.5, 12-PR) tested at three inflation pressures (104, 207, and 414 kN/m²) and under wheel loads ranging from 6670 to 20,030 N were investigated. Stresses and displacements were computed by the theory of elasticity for various depths in the half-space under loading conditions: measured, assumed uniform, assumed parabolic, and assumed conical pressure distributions. Generally, the assumption of uniform pressure distribution was found to be unreasonable in cases of high-inflated tires on a hard surface and on sands, but it was found acceptable in the other investigated cases, including those for clay surfaces. However, the assumption of parabolic pressure distribution was found to be more realistic than that of a uniform one for high-inflated tires on sands and for low-inflated tires with light load on loose sand.

DD FORM 1473

REPLACES DD FORM 1473, 1 JAN 64, WHICH IS OBSOLETE FOR ARMY USE.

ja

Unclassified
Security Classification

14. KEY WORDS	LINK A		LINK B		LINK C	
	ROLE	WT	ROLE	WT	ROLE	WT
Elastic media Pneumatic tire Pressure distribution Soil stresses Tires						

TA7
W34m
No. M-70-6

THE CONTENTS OF THIS REPORT ARE NOT TO BE
USED FOR ADVERTISING, PUBLICATION, OR
PROMOTIONAL PURPOSES. CITATION OF TRADE
NAMES DOES NOT CONSTITUTE AN OFFICIAL EN-
DORSEMENT OR APPROVAL OF THE USE OF SUCH
COMMERCIAL PRODUCTS.

Foreword

The study reported herein was conducted at the U. S. Army Engineer Waterways Experiment Station (WES) as a part of the vehicle mobility research program under Department of the Army Project 1T061102B52A, "Research in Military Aspects of Terrestrial Sciences," Task 01, "Terrain Aspects of Off-Road Mobility," under the sponsorship and guidance of the Directorate of Development and Engineering, U. S. Army Materiel Command.

Data for this study were collected from tests previously conducted by Mobility Research Branch (MRB) personnel at the WES. The study was conceived and carried out by Dr. Y. T. Chou under the general supervision of Messrs. W. G. Shockley and S. J. Knight, Chief and Assistant Chief, respectively, of the Mobility and Environmental Division, and Dr. D. R. Freitag, former Chief, MRB, and now Chief, Office of Technical Programs and Plans, WES, and under the direct supervision of Dr. K. W. Wiendieck, MRB. Dr. Chou prepared this report.

COL Levi A. Brown, CE, was Director of WES during the course of this study. Messrs. J. B. Tiffany and F. R. Brown were Technical Directors.

Contents

	<u>Page</u>
Foreword	v
Notation	ix
Conversion Factors, Metric to British	
Units of Measurement	xi
Summary	xiii
Background	1
Purpose	1
Scope	2
Basic Equations Used in the Analysis	2
Computational Procedure	5
Measured pressure distributions	5
Assumed pressure distributions	7
Analysis and Discussion of Results	7
Results for tests on firm surfaces	9
Results for tests in soft soils	11
Computations for assumed conical and parabolic pressure patterns	13
Conclusions	14
Literature Cited	15
Tables 1-2	
Plates 1-10	

Notation

- a Length of a rectangular area; radius of a circle
- A A parameter in equation 2b
- b Width of a rectangular area
- B A parameter in equation 2b
- E Young's modulus
- m A parameter in equation 2b
- n A parameter in equation 2b
- P Concentrated normal pressure
- q Unit normal pressure on the surface of the medium
- r Radial distribution in a cylindrical coordinate system
- w Displacement
- z Depth
- σ_z Vertical stress
- ν Poisson's ratio

Conversion Factors, Metric to British Units of Measurement

Metric units of measurement used in this report can be converted to British units as follows:

<u>Multiply</u>	<u>By</u>	<u>To Obtain</u>
centimeters	0.3937	inches
newtons	0.2248	pounds (force)
kilonewtons per square meter	0.145	pounds per square inch

Summary

The validity of the assumption of uniform pressure distribution under a pneumatic tire was checked in this study. Measurements of pressure distributions under pneumatic tires at their interface with firm surfaces and soft soils, previously made at the U. S. Army Engineer Waterways Experiment Station, were used. Two tires (11.00-20, 12-PR, and 12-22.5, 12-PR) tested at three inflation pressures (104, 207, and 414 kN/m²) and under wheel loads ranging from 6670 to 20,030 N were investigated. Stresses and displacements were computed by the theory of elasticity for various depths in the half-space under loading conditions: measured, assumed uniform, assumed parabolic, and assumed conical pressure distributions.

Generally, the assumption of uniform pressure distribution was found to be unreasonable in cases of high-inflated tires on a hard surface and on sands, but it was found acceptable in the other investigated cases, including those for clay surfaces. However, the assumption of parabolic pressure distribution was found to be more realistic than that of a uniform one for high-inflated tires on sands and for low-inflated tires with light load on loose sand.

EFFECT OF PRESSURE DISTRIBUTION UNDER PNEUMATIC TIRES ON
STRESSES AND DISPLACEMENTS IN THE SUPPORTING ELASTIC MEDIA

Background

1. In analytic studies of pavement structural design, a common assumption has been that vehicle tires transmit uniformly distributed pressure to the supporting medium over a circular area.¹ This assumption, which results in mathematical convenience and simplification, also has been made² in the studies of off-road soil-vehicle relations that have been developing rapidly in recent years. However, the pressure distribution pattern beneath a pneumatic tire is seldom uniform and depends upon a number of factors, i.e. the magnitude of the load, geometry and rigidity of the tire, and the characteristics of the supporting medium. Experimental studies on firm and soft surfaces conducted at the U. S. Army Engineer Waterways Experiment Station (WES)^{3,4,5} have shown that the pressure distribution pattern is approximately uniform only when the tire-inflation pressure is very low, the tire walls are very flexible, and the supporting medium (soil) is very soft.

2. The magnitudes of stresses and displacements in pavement induced by surface loading have influence upon the pavement design. Since the stresses and displacements within the supporting medium depend upon the pressure distribution induced at the surface and since the pressure distribution pattern under a tire is known to be nonuniform, the question arose as to the magnitude of the calculated deviation in stress and strain within the medium caused by the simplified assumption of uniform distribution.

Purpose

3. The purpose of this study was to determine the effect of various measured pressure distributions under pneumatic tires on the stresses and displacements at points beneath the centroid of the pressure distributions within an elastic half-space,* as a possible means of

* In general, all considerations and conclusions pertaining to the elastic half-space refer to the centroid line only.

obtaining qualitative estimates of the error induced by simple assumed pressure distributions.

Scope

4. Existing pressure distribution data from previous WES tests with 12-ply rating tires commonly used on military land vehicles were considered for the analysis. These data were obtained by using stress cells.^{3,4,5} Pertinent test parameters are summarized in table 1. Representative stress maps are presented in plate 1.

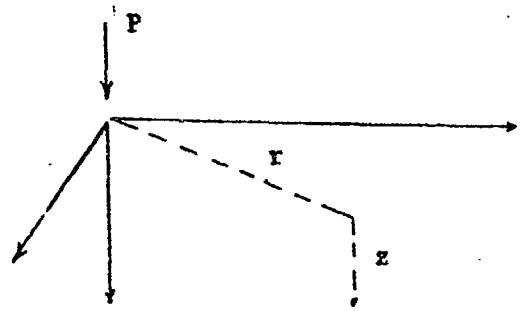
5. Stresses and displacements at various depths beneath the centroid of the pressure distributions were computed by the theory of elasticity for cases of measured and assumed pressure distributions, and the results were compared. The computations for the assumed uniform pressure distributions were based on circular and rectangular contact areas. Also, assumed conical and parabolic pressure distributions over circular contact areas were investigated. These combinations of areas and pressure distributions represent some of the simpler cases. In fact, test results show that under high-inflated tires the pressure tends to concentrate in the central portion of the tire, so the pressure distribution pattern is nearly parabolic.

Basic Equations Used in the Analysis

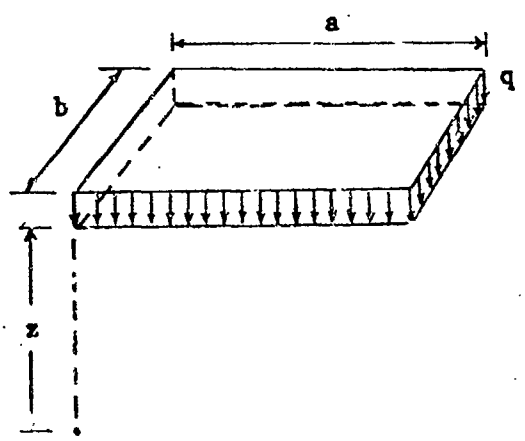
6. Vertical stress and vertical displacement under a point load (fig. 1a) were needed to analyze the measured irregular pressures. They were computed by the following equations:⁶

$$\sigma_z = \frac{3P}{2\pi} \frac{z^3}{(r^2 + z^2)^{5/2}} \quad (1a)$$

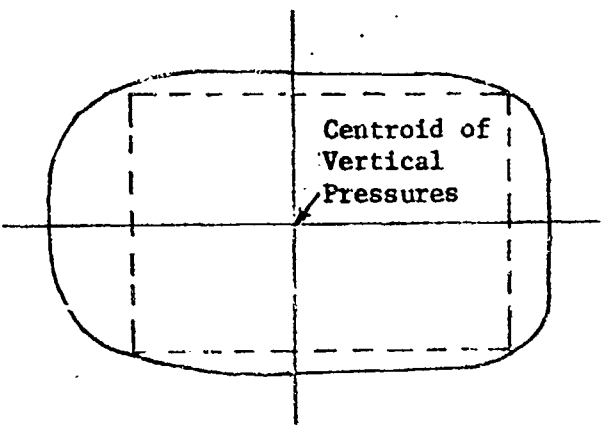
$$w = \frac{P(1+\nu)}{2\pi E} \left[\frac{z^2}{(r^2 + z^2)^{3/2}} + \frac{2(1-\nu)}{(r^2 + z^2)^{1/2}} \right] \quad (1b)$$



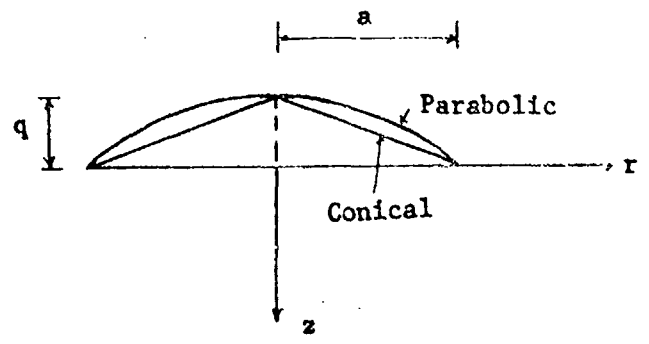
a. UNDER A POINT LOAD



b. UNDER CORNER OF UNIFORMLY LOADED RECTANGULAR AREA



c. UNDER CENTROID OF MEASURED PRESSURE DISTRIBUTION



d. UNDER CIRCULAR AREA WITH CONICAL AND PARABOLIC PRESSURE DISTRIBUTIONS

Fig. 1. Schematic of assumed pressure distributions

7. Vertical stress and vertical displacement under the corner of a uniformly loaded rectangular area (fig. 1b) were needed to compute stresses and displacements beneath the centroid of measured pressure distributions (fig. 1c). They were computed by the following equations:⁶

$$\sigma_z = \frac{q}{2\pi} \left[\frac{mn}{\sqrt{1+m^2+n^2}} \frac{1+m^2+2n^2}{(1+n^2)(m^2+n^2)} + \sin^{-1} \frac{m}{\sqrt{m^2+n^2}\sqrt{1+n^2}} \right] \quad (2a)$$

$$w = \frac{aq}{2E}(1-\nu^2) \left(A - \frac{1-2\nu}{1-\nu} \right) B \quad (2b)$$

where

$$A = \frac{1}{\pi} \left(\ln \frac{\sqrt{1+m^2+n^2} + m}{\sqrt{1+m^2+n^2} - m} + m \ln \frac{\sqrt{1+m^2+n^2} + 1}{\sqrt{1+m^2+n^2} - 1} \right)$$

$$B = \frac{n}{\pi} \tan^{-1} \frac{m}{n\sqrt{1+m^2+n^2}}$$

$$m = \frac{b}{a}$$

$$n = \frac{z}{a}$$

8. Vertical stress and vertical displacement under the center of a uniformly loaded circular area (fig. 1d) were computed by the following equations:⁶

$$\sigma_z = q \left\{ 1 - \frac{1}{[(a/z)^2 + 1]^{3/2}} \right\} \quad (3a)$$

$$w = \frac{2aq(1-\nu^2)}{E} (\sqrt{1+n^2} - n) \left[1 + \frac{n}{2(1-\nu)\sqrt{1+n^2}} \right] \quad (3b)$$

9. Vertical stress under the center of a circular area with conical pressure distribution (fig. 1d) was computed by the following

equation:⁷

$$\sigma_z = q \left\{ 1 - \frac{1}{\left[\left(\frac{a}{z} \right)^2 + 1 \right]^{1/2}} \right\} \quad (4)$$

10. Vertical stress under the center of a circular area with parabolic pressure distribution (fig. 1d) was computed by the following equation:⁷

$$\sigma_z = q \left[\frac{1}{\frac{z}{a} + \sqrt{1 + \left(\frac{z}{a} \right)^2}} \right]^2 \left[\frac{2 \left(\frac{z}{a} \right)}{1 + \sqrt{1 + \left(\frac{z}{a} \right)^2}} \right] \quad (5)$$

11. The above equations were numerically solved with a General Electric 200 computer at the WES. Poisson's ratio was assumed to be $\nu = 0.25$.

12. Since equations 1-5 were derived from the theory of linear elasticity, they can be used only for elastic materials such as steel or, to a lesser extent, concrete mixtures and asphalt mixtures. Therefore, the computed results or conclusions presented herein that are based on pressure distribution on a firm surface may be applied only to problems involving supporting materials composed of hard rocks, concrete, or asphalt mixtures. Unfortunately, such materials as sands and clays behave in a very complicated, nonlinear manner, and their true behavior beneath a tire may not conform with the theory of elasticity. Hence, the results in this study concerning soft soils, i.e. sands and clays, can be used only as a first approximation of the true solution. However, this study should provide an insight into the problem.

Computational Procedure

Measured pressure distributions

13. Stresses and displacements were computed for various points

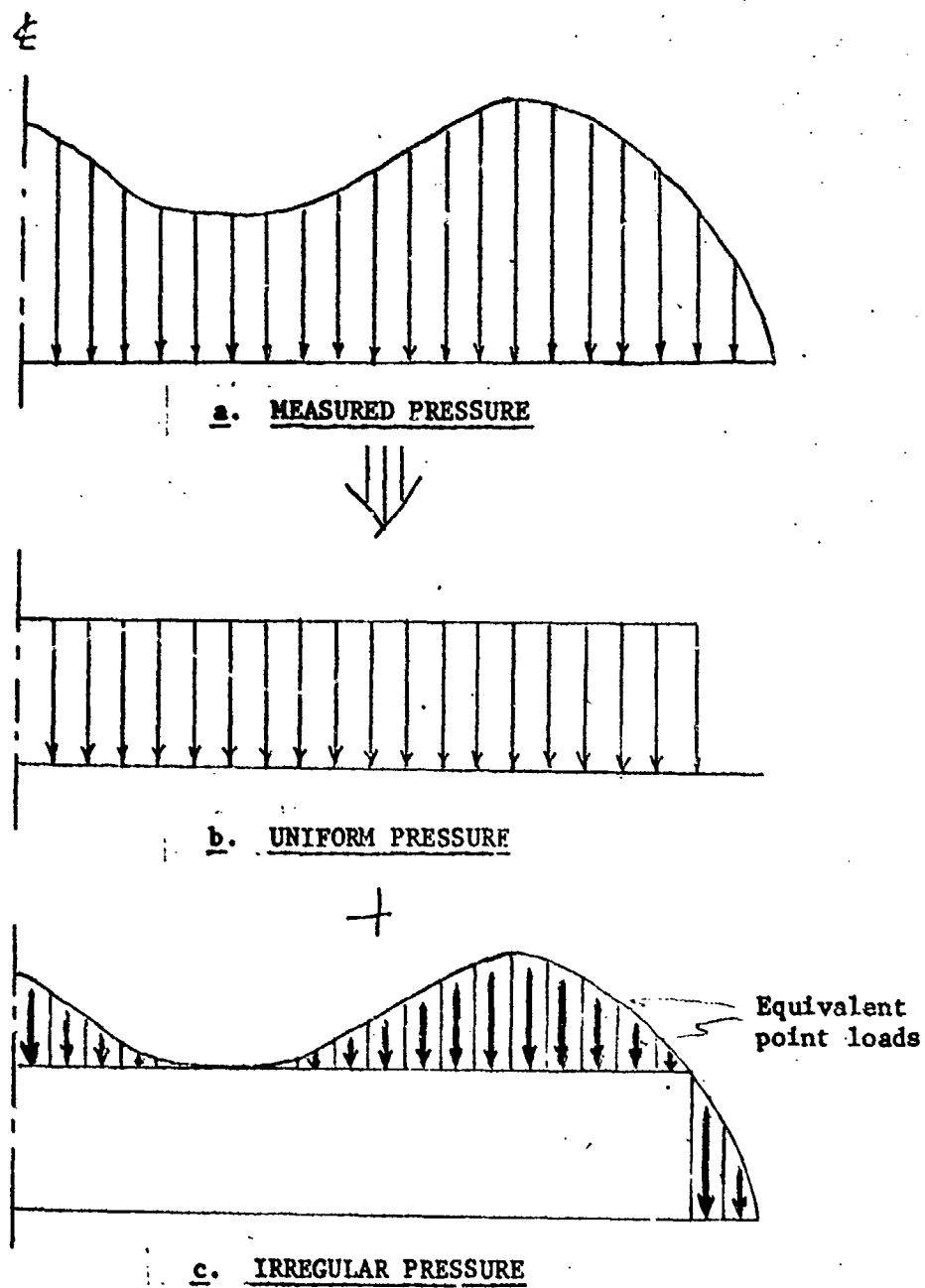


Fig. 2. Schematic division of measured pressure distribution

along the vertical axis originating at the centroid of the vertical pressures. Since the measured pressure distribution under a tire is not expressed analytically, an approximation procedure was applied to use the above-listed equations. The actual pressure diagram (fig. 2a) was separated into two portions: (a) uniformly distributed pressures over a rectangular area within the actual tire print (fig. 2b), and (b) the remaining irregular pressures over the total tire print that are further replaced by a number of equivalent point loads (fig. 2c). In this manner the accuracy of the procedure was increased because exact equations 2a and 2b were applied to the portion with uniform pressure distribution, while the approximation was restricted to the remaining portion. Total stress or displacement induced by actual loads is the sum of those induced by the two portions.

14. For the irregular part of the pressure distribution, the tire print was divided into many small areas, depending upon smoothness of the pressure distribution, e.g. the low-inflated, treaded tires on firm surfaces were divided into approximately 1000 areas, which was about the greatest number used. The sum of irregularly and uniformly distributed pressures should theoretically equal the actual tire load. When the difference between the load obtained by the summing procedure and the actual load exceeded about 10-15 percent, the entire procedure was repeated with a refined subdivision of the area of irregular pressure.

Assumed pressure distributions

15. For uniform pressure distribution, the idealized rectangular and circular contact areas had the same area as the actual tire prints. For uniformly loaded rectangular areas, the widths were chosen equal to those of the actual tire prints, and the lengths were computed so as to obtain the same areas.

Analysis and Discussion of Results

16. Computed results, in terms of σ_z and w , were very close for assumed uniformly distributed pressures over the circular and rectangular areas considered, the difference being less than 5 percent in most cases.

Because of this small difference, and also since most tire prints are between rectangular and elliptical in shape rather than circular, emphasis was placed on comparing results obtained under actual loads with those obtained under assumed uniform pressure distributions over rectangular areas. For convenience of presentation, the computed results were expressed as ratios of assumed-to-measured condition, and the ratios were plotted for various depths (plates 2-10). In so doing, Young's modulus E in the equations was cancelled, and the results were expressed as dimensionless numbers.

17. The inset drawings in plates 2-10 depict the measured pressure distributions beneath a tire. They are plotted along the center line (solid line) of the tire print and along an offset line (dot-dash line). The equivalent uniformly distributed pressures are also plotted (dashed line) for comparison. In most cases, the difference between stresses and displacements induced by measured and uniform pressure distributions can be anticipated from these drawings. When the pressure is concentrated at regions near the center of the contact area (for example, see plate 6c), the corresponding stresses and displacements along the centroid line within the elastic half-space are greater than those induced by the equivalent uniform pressure distribution (stress and displacement ratios are less than 1.0).

18. The equivalent uniform pressure distribution has been determined from the three-dimensional shape of the measured distribution. Therefore, the area inclosed by a rectangle (the uniform pressure distribution) in the longitudinal direction on the inset drawings is not equal to the area inclosed by the measured pressure wave at the center line (or the offset line). Similarly, the area inclosed by a rectangle in the lateral direction, as shown at the left-hand side of the inset drawings, is not equal to the area inclosed by the measured pressure distribution. It also should be pointed out that the pressure distribution in the longitudinal direction of the tire is not necessarily symmetrical, and the peak pressure along the lateral axis across the centroid of the pressure pattern may be different from those along other parallel axes.

19. The difference in the computed results (stresses and displacements) of the uniform and measured pressure distributions shown in the plates is large near the surface, but decreases as the depth increases. This may be explained by the principle of Saint Venant,⁸ which states, "If the forces acting on a small portion of the surface of an elastic body are replaced by another statically equivalent system of forces acting on the same portion of the surface, this redistribution substantially changes the stresses locally, but has a negligible effect on the stresses at distances that are large in comparison with the linear dimensions of the surface on which the forces are changed."

20. Worthy of note is the fact that differences in stress are much more pronounced than those in displacements. The stresses at a certain point on the surface and in a region close to that point are influenced more than the displacements are by the intensity of the pressure at or near the point. In an extreme case, the vertical stress at a point on the surface is zero if the pressure is not directly acting upon the point, but the displacement for the same case is not zero.

Results for tests on firm surfaces

21. The stress and displacement ratios for an 11.00-20 smooth, towed tire at three different inflation pressures and loaded to 13,350 N are shown in plate 2. The contact area of the tire was larger and the zone of high edge pressure was more pronounced at low tire-inflation pressures than at high inflation pressures. The pressure at the center of the tire for the measured pressure distribution was less than that under uniform pressure. As the inflation pressure increased, the peak pressure under the tire tended to move to the center, and the pressure intensity at the center of the tire print became greater for the measured pressure distribution than that under the equivalent uniform pressure. At high tire-inflation pressure, the pressure near the edge of the tire was still greater than that at the point halfway between the center and the edge of the tire. This was caused primarily by the sidewall rigidity of the test tire (ply rating = 12). The plotted curves in plate 2 show that the computed stress ratios were much higher than unity for a low-inflated tire; the situation was reversed for a high-inflated

tire. In the latter case, the vertical stress on the surface under uniform pressure was 66 percent of the stress induced by the measured pressure distribution. The computed displacement ratios for a low-inflated tire were near unity, but were less than unity for a high-inflated tire; however, the difference was not large within the test range.

22. Results are shown in plate 3 for the same tire under static conditions. The pressure distribution patterns are very similar to those in plate 2, and the computed results are quite close to those for the rolling tire.

23. Computed results for a 12-22.5 treaded, tubeless tire in the static condition and loaded to 12,450 N are shown in plate 4. The highly irregular pressure distribution pattern under the tire was caused by treads with zigzag shape. It is interesting to note that the vertical pressure distribution along the lateral axis through the centroid of this truck-mounted tire was markedly asymmetrical, especially at the lowest inflation pressure. The other tires in this study were mounted on the single-wheel test carriage and produced symmetrical patterns at all tire pressures. The asymmetry of the truck-mounted tire had no bearing on the analysis of data in this study; however, the magnitude of the disparity in peak pressures (at the lowest inflation pressure, the peak pressure was 600 kN/m^2 on the outside and 400 kN/m^2 on the inside of the tire) was sufficiently great to suggest that this phenomenon be investigated further at the first opportunity.

24. The pressure distributions shown in plate 4 generally are similar to those in plates 2 and 3, except for the irregular appearance caused by the treads. The computed results for the cases represented in these three plates are also quite close. As seen in plate 4, the computed ratios for stresses and displacements were close to unity at inflation pressures of 104 and 207 kN/m^2 , but at 414 kN/m^2 the ratios were much less than unity. In the case of vertical stress, the computed results on the surface under uniform pressures were only 63 percent of the stresses induced by the measured pressure distributions.

Results for tests in soft soils

25. Computed results for towed tires on sand and clay are plotted in plates 5-10. As stated previously, these results, derived by the theory of elasticity, can be viewed only as a qualitative first approximation of the desired solution; any attempt to explain the computed results on a quantitative basis probably would be misleading.

26. Tests on sand. Results for a low-inflated (104 kN/m^2) tire loaded to 13,350 N and towed over sand of three different strengths are shown in plate 5. The sand conditions ranged from loose to dense. Edge stresses here were significant for all sand strengths tested, which again was caused by the sidewall rigidity of the test tire. As shown in plate 5, the contact length decreased with penetration resistance, but the contact width increased. Double peaks in the pressure distribution along the center line were common, but were found at the offset line in dense sand only.

27. The stress ratios in plate 5 were much greater than unity when the supporting sand had high penetration resistance values, but decreased and became less than unity when the penetration resistance values decreased. The displacement ratios were near unity for high penetration resistance values, but became less than unity as the penetration resistance values decreased. The computed stress and displacement ratios were observed to be near unity when double peaks of pressure along both the tire center line and the offset line occurred.

28. Results in plate 6 are from tests conducted under similar conditions as those represented in plate 5, the only difference being the higher tire-inflation pressure (414 kN/m^2) for the tests in plate 6. Double peaks and edge stresses were not observed. The pressure distributions have shapes similar to a parabola.

29. In general, the pressure patterns under the high-inflated tire on sands of different strengths were very similar to each other, but they were quite different from those under the low-inflated tire (plate 5). This may be explained qualitatively by the fact that relatively high-inflated tires almost behave like rigid wheels, experiencing little deformation and relatively high sinkage, while low-inflated tires undergo

greater deformation (providing greater contact area) and relatively little sinkage. The computed stress and displacement ratios for high-inflated tires (plate 6) were much less than unity; therefore, the assumption of uniform pressure distribution under a high-inflated tire on sand appears to be unreasonable.

30. The results for a low-inflated (104 kN/m^2) tire towed over a loose sand under three different loads are shown in plate 7. The patterns of the pressure distribution fall between those of plates 5 and 6. For the heaviest load tested (20,030 N), double peaks of pressure were observed at both the tire center line and the offset line; the pressure distributions along these lines were quite similar and relatively uniform. For the medium load (13,350 N), the pressure distribution along the center line was similar to that at 20,030 N, but the pressure distribution along the offset line presented only one peak near the center. For the smallest load (6670 N), the pressure distributions were approximately parabolic in the longitudinal direction, but edge stresses were observed. Results plotted in plate 7 show that the computed stress and displacement ratios near the surface were close to unity under heavy loads, but became less than unity as the load was decreased. Therefore, the assumption of uniform pressure distribution under a low-inflated tire on loose sand may be justified.

31. Results in plate 8 refer to test conditions similar to those represented in plate 7, the difference being the higher inflation pressure (414 kN/m^2) for the results in plate 8. The pressure patterns are very much like those in plate 6 in that the pressure distribution along the lateral section of the tire was quite uniform at the central portion of the tire and then decreased gradually to the ends. Again as anticipated, the computed stress and displacement ratios were much less than unity. This is confirmed by the plotted results in plate 8.

32. Tests in clay. Available pressure distribution data from tests on clay were not as numerous as those on sand. Results for tests with a tire loaded to 13,350 N and towed over a soft clay at three different inflation pressures are shown in plate 9. Zones of slightly higher edge pressures can be seen, but they are not located as close to the edge of

the tire as they were in sand and on a firm surface. In general, the pressures beneath the tire were distributed more uniformly in clay than in sand.

33. The plotted results show that at low inflation pressure, the computed stress and displacement ratios were near unity, but tended to become less than unity as the inflation pressure increased; so the assumption of uniform pressure distribution is not justified for a high-inflated tire on clay.

34. Results from tests conducted under conditions similar to those represented in plate 9 are shown in plate 10, but the wheel load was 6670 N for the tests in plate 10. Test data for an inflation pressure of 414 kN/m^2 were not complete and so are not shown in the plate. Under tires with low tire-inflation pressures and light load, zones of edge stress were again observed as in sand. The plotted curves for the computed results indicate that the stress and displacement ratios were not very much less than unity, and the assumption of uniform pressure distribution thus appears reasonable.

Computations for assumed conical and parabolic pressure patterns

35. Computed ratios of vertical stress at three different depths for equivalent conical and parabolic pressure distributions are listed in table 2. The stresses computed for the conical distributions were greater than those computed for the measured pressure distributions in all cases analyzed.

36. The stresses computed for measured pressure distributions on a firm surface tended to draw closer to those computed for the equivalent parabolic pressures as the tire-inflation pressure was increased. For the cases analyzed at high inflation pressure (414 kN/m^2), uniform pressure appears to be more realistic than the parabolic one. For measured pressure distributions in sand, the computed stresses were close to those computed for the parabolic pressure distributions for high-inflated (414 kN/m^2) tires; however, for low-inflated (104 kN/m^2) tires, this conclusion applies only to loose sand and light load. In these cases, the parabolic pressure distributions appear to be more realistic than uniform pressure distributions.

Conclusions

37. Because the analysis herein is based on limited data, conclusions are not drawn on a quantitative basis. Nevertheless, for the analyzed conditions, it is concluded that:

- a. The computed stresses and displacements under measured pressure distributions are different from those under equivalent uniform pressures. The difference is most significant at shallow depths, but becomes negligibly small as depth increases.
- b. Under pressure distributions produced by high-inflated tires on a firm surface, the computed stresses are larger than those produced by the equivalent uniform pressure. Under low-inflated tires, the situation is reversed.
- c. The computed results for smooth and treaded tires on a firm surface are not significantly different.
- d. Under pressure distributions produced by high-inflated tires on sand, the computed stresses and displacements are much larger than those computed for the equivalent uniform pressures.
- e. Under pressure distributions produced by low-inflated tires on dense sand, the computed stresses under measured pressure distributions are smaller than those computed for the equivalent uniform pressures. For pressure distributions on loose sand, the difference in stresses and displacements is insignificant, except under a light load. Under a light load, the computed stresses and displacements under measured pressure distributions are much greater than those under the equivalent uniform pressures.
- f. The above conclusions apply to assumed equivalent uniform pressure distributions on both circular and rectangular contact areas. The computed results for both contact areas differ by not more than 5 percent.
- g. The stresses computed for the assumed conical and parabolic

pressure distributions are, in general, much larger than those for the measured pressure distributions. The computed stresses for measured pressure distributions on a firm surface tend to draw closer to those computed for the equivalent parabolic pressures as the tire-inflation pressure increases. For measured pressure distributions in sand, the computed stresses are close to those computed for the parabolic pressures in cases of high-inflated tires; but in cases of low-inflated tires only on loose sand and under light loads (table 2). In these cases, the parabolic distributions appear to be more reasonable than uniform pressure distributions.

Literature Cited

1. Yoder, E. J., Principles of Pavement Design, Wiley, New York, 1959.
2. Kraft, D. C., "Analytical Landing Gear - Soils Interaction - Phase I," Technical Report AFFDL-TR-68-88, Aug 1968, Air Force Flight Dynamics Laboratory, Wright-Patterson Air Force Base, Ohio.
3. Green, A. J., McRae, J. L., and Murphy, N. R., "Stresses Under Moving Vehicles; Distribution of Stresses on an Unyielding Surface Beneath Stationary and Towed Pneumatic Tires," Technical Report No. 3-545, Report 4, Jul 1964, U. S. Army Engineer Waterways Experiment Station, CE, Vicksburg, Miss.
4. Green, A. J., and Murphy, N. R., "Stresses Under Moving Vehicles; Distribution of Stresses Beneath a Towed Pneumatic Tire in Air-Dry Sand," Technical Report No. 3-545, Report 5, Jul 1965, U. S. Army Engineer Waterways Experiment Station, CE, Vicksburg, Miss.
5. Freitag, D. R., Green, A. J., and Murphy, N. R., "Normal Stresses at the Tire-Soil Interface in Yielding Soils," Miscellaneous Paper No. 4-629, Feb 1964, U. S. Army Engineer Waterways Experiment Station, CE, Vicksburg, Miss.
6. Harr, M. E., Foundations of Theoretical Soil Mechanics, McGraw-Hill, New York, 1966.
7. Harr, M. E., and Lovell, C. W., "Vertical Stresses Under Certain Axisymmetrical Loadings," Stresses in Soils and Layered Systems, HRB Record 39, pp 68-81, 1963, Highway Research Board, Washington, D. C.

8. Timoshenko, S., and Goodier, J. N., Theory of Elasticity, 2d Ed, McGraw-Hill, New York, 1951.

Table 1

Pressure Distribution Test Data

Identifi- cation No.*	Test Medium	Penetration Resistance, kN/m ²		Size	Type	Test Condi- tion	Load, N	Infl Press, kN/m ²	Plate No.**	Test No.
		0-15 cm	15-30 cm							
1	Firm surface ↓ Sand ↓ Clay ↓	-	-	11.00-20, 12-PR	Buffed smooth	Towed	13,350	104	2	-
2		-	-	11.00-20, 12-PR	Buffed smooth	Towed	13,350	207	2	-
3		-	-	11.00-20, 12-PR	Buffed smooth	Towed	13,350	414	2	-
4		-	-	11.00-20, 12-PR	Buffed smooth	Static	12,370	104	3	-
5		-	-	11.00-20, 12-PR	Buffed smooth	Static	12,370	207	3	-
6		-	-	11.00-20, 12-PR	Buffed smooth	Static	12,370	414	3	-
7†		-	-	12-22.5, 12-PR	Treaded	Static	12,450	104	4	-
8†		-	-	12-22.5, 12-PR	Treaded	Static	12,450	207	4	-
9†		-	-	12-22.5, 12-PR	Treaded	Static	12,450	414	4	-
10		393	1600	11.00-20, 12-PR	Buffed smooth	Towed	13,350	104	5	34
11		207	968	11.00-20, 12-PR	Buffed smooth	Towed	13,350	104	5	35
12		131	345	11.00-20, 12-PR	Buffed smooth	Towed	13,350	104	5	23
13		371	1155	11.00-20, 12-PR	Buffed smooth	Towed	13,350	414	6	33
14		186	645	11.00-20, 12-PR	Buffed smooth	Towed	13,350	414	6	31
15		110	336	11.00-20, 12-PR	Buffed smooth	Towed	13,350	414	6	27
16		116	364	11.00-20, 12-PR	Buffed smooth	Towed	20,030	104	7	30
17		131	345	11.00-20, 12-PR	Buffed smooth	Towed	13,350	104	7	25
18		124	324	11.00-20, 12-PR	Buffed smooth	Towed	6,670	104	7	22
19		117	372	11.00-20, 12-PR	Buffed smooth	Towed	20,030	414	8	28
20		110	336	11.00-20, 12-PR	Buffed smooth	Towed	13,350	414	8	27
21		110	336	11.00-20, 12-PR	Buffed smooth	Towed	6,670	414	8	24
22		275	-	11.00-20, 12-PR	Buffed smooth	Towed	13,350	104	9	B-7
23		323	-	11.00-20, 12-PR	Buffed smooth	Towed	13,350	207	9	B-6
24		310	-	11.00-20, 12-PR	Buffed smooth	Towed	13,350	414	9	B-5
25		303	-	11.00-20, 12-PR	Buffed smooth	Towed	6,670	207	10	B-10
26		296	-	11.00-20, 12-PR	Buffed smooth	Towed	6,670	104	10	B-11

* Identification numbers refer to the same numbers in table 2.

** These numbers refer to the plate numbers in this report.

† These tests were run with the tire mounted on a truck; all other tests were conducted in the single-

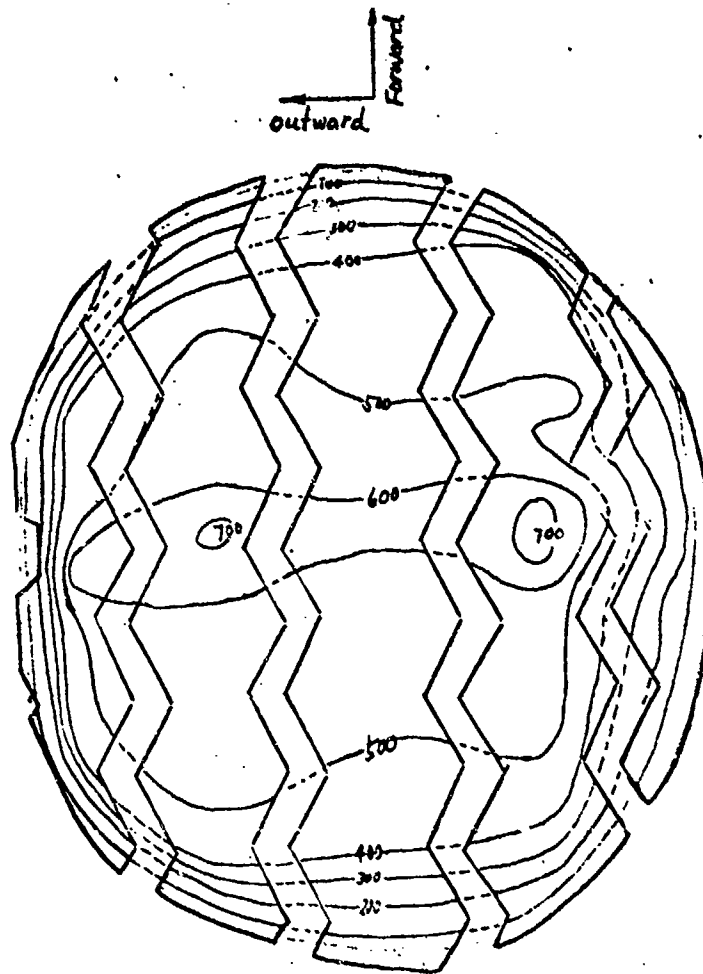
wheel test carriage in the URS Mobilizer Research Branch

Table 2

Computed Stress Ratios in Conical and Parabolic Pressure Patterns

Identifi- cation No.*	Depth cm	Stress Ratios		Identifi- cation No.*	Depth cm	Stress Ratios	
		Cone/ Measured	Parabola/ Measured			Cone/ Measured	Parabola/ Measured
1	0	3.20	2.14	13	0	1.27	0.85
	5	1.84	1.51		5	1.05	0.86
	15	1.09	1.02		15	0.96	0.90
2	0	2.95	1.96	14	0	1.27	0.85
	5	1.83	1.54		5	1.13	0.90
	15	1.18	1.12		15	0.92	0.84
3	0	2.05	1.36	15	0	2.01	1.34
	5	1.62	1.41		5	1.38	1.12
	15	1.18	1.14		15	1.14	1.06
4	0	2.88	1.92	16	0	3.36	2.24
	5	2.53	2.10		5	2.48	1.94
	15	1.45	1.37		15	1.53	1.38
5	0	2.58	1.72	17	0	1.72	1.15
	5	2.00	1.70		5	1.18	0.96
	15	1.27	1.22		15	0.96	0.89
6	0	2.30	1.54	18	0	1.60	1.07
	5	1.44	1.25		5	1.23	0.99
	15	1.17	1.07		15	1.05	0.97
7	0	2.45	1.63	19	0	2.17	1.44
	5	1.84	1.56		5	1.47	1.20
	15	1.23	1.17		15	1.20	1.12
8	0	2.75	1.83	20	0	3.50	2.31
	5	1.74	1.50		5	2.10	1.69
	15	1.14	1.10		15	1.42	1.31
9	0	2.14	1.43	21	0	2.69	1.80
	5	1.36	1.18		5	1.79	1.45
	15	1.07	1.04		15	1.35	1.26
10	0	5.22	3.48	22	0	2.45	1.63
	5	3.02	2.43		5	1.80	1.46
	15	1.48	1.36		15	1.40	1.31
11	0	3.49	2.33	23	0	2.14	1.43
	5	2.16	1.71		5	1.48	1.24
	15	1.26	1.15		15	1.06	1.01
12	0	2.61	1.74	24	0	2.19	1.46
	5	1.87	1.46		5	1.11	0.94
	15	1.22	1.10		15	0.99	0.93

* Identification numbers refer to the same numbers in table 1.



12x22.5, 12 PR tubeless tire

414 $\frac{\text{kg}}{\text{m}^2}$ inflation pressure

12,450-N static load on hard surface

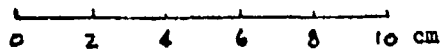
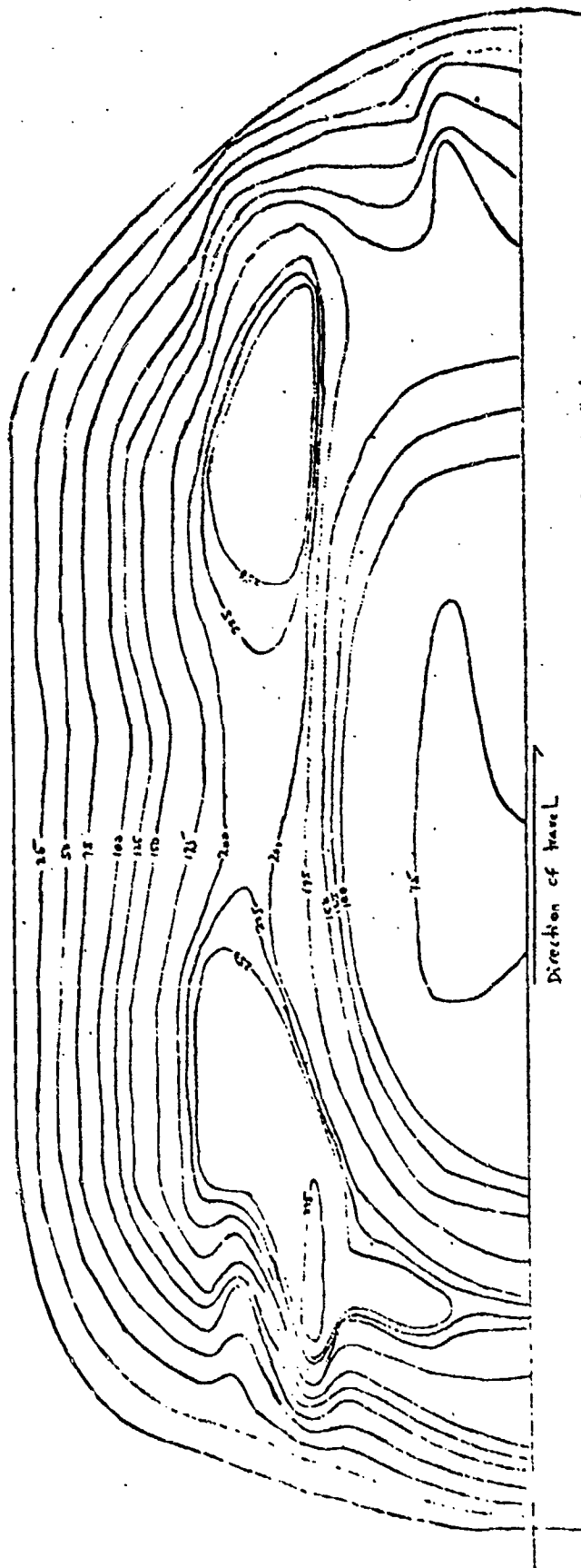


PLATE 1A



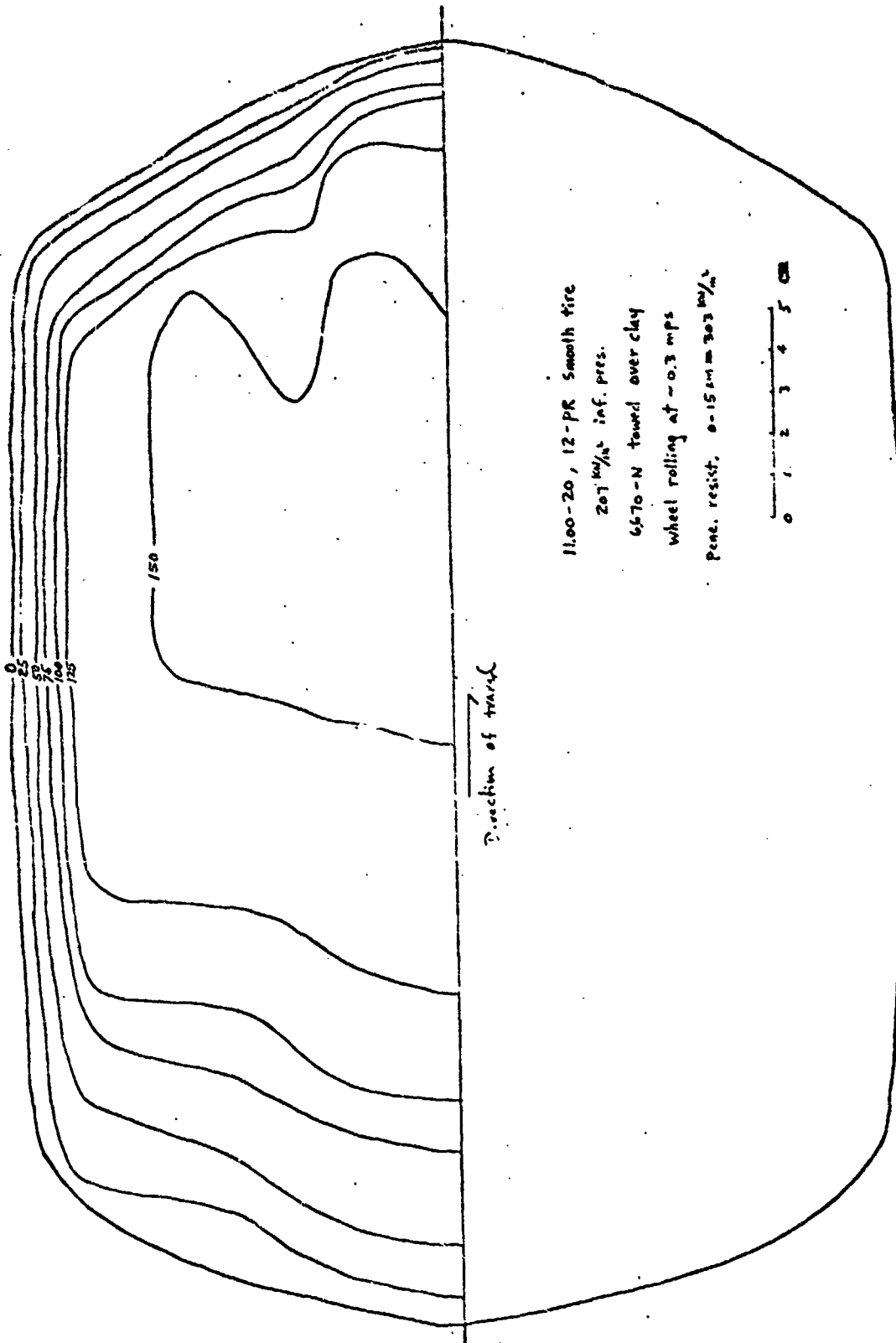
11.00-20, 12 PR. Smooth fine
 104 $\frac{1}{2}$ in. Inf. pres.
 17350-4 fluted wheel over sand
 wheel rolling at 0.7 mps
 Pres. result. 6-15 to 200 $\frac{1}{2}$ in.
 15-30 cm in 60 $\frac{1}{2}$ in.



Direction of travel

20

PLATE 1B

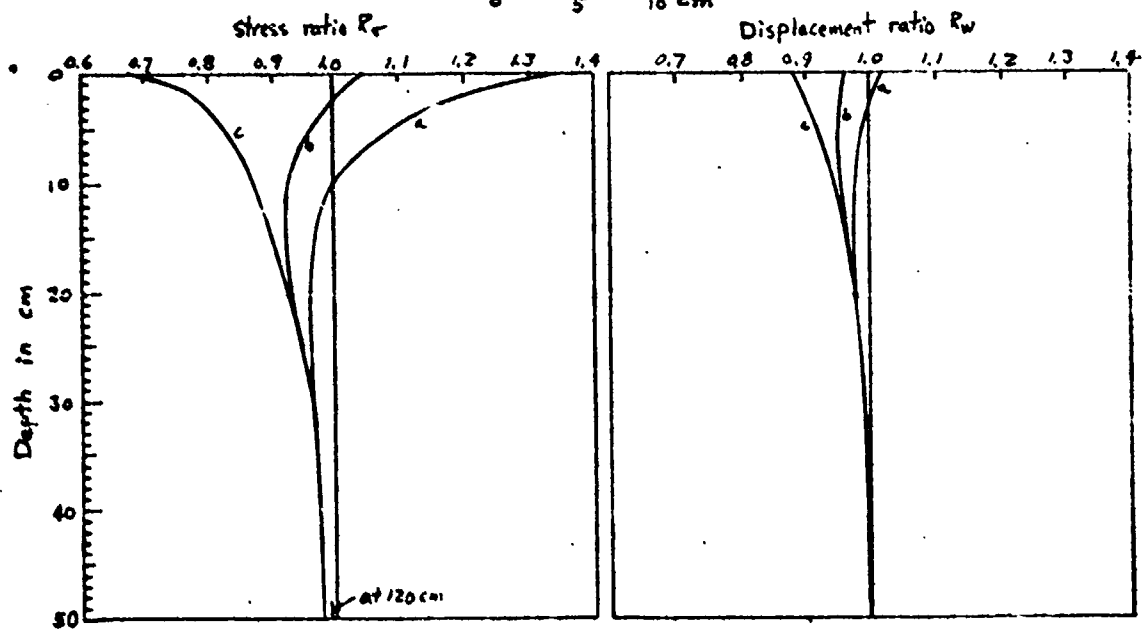
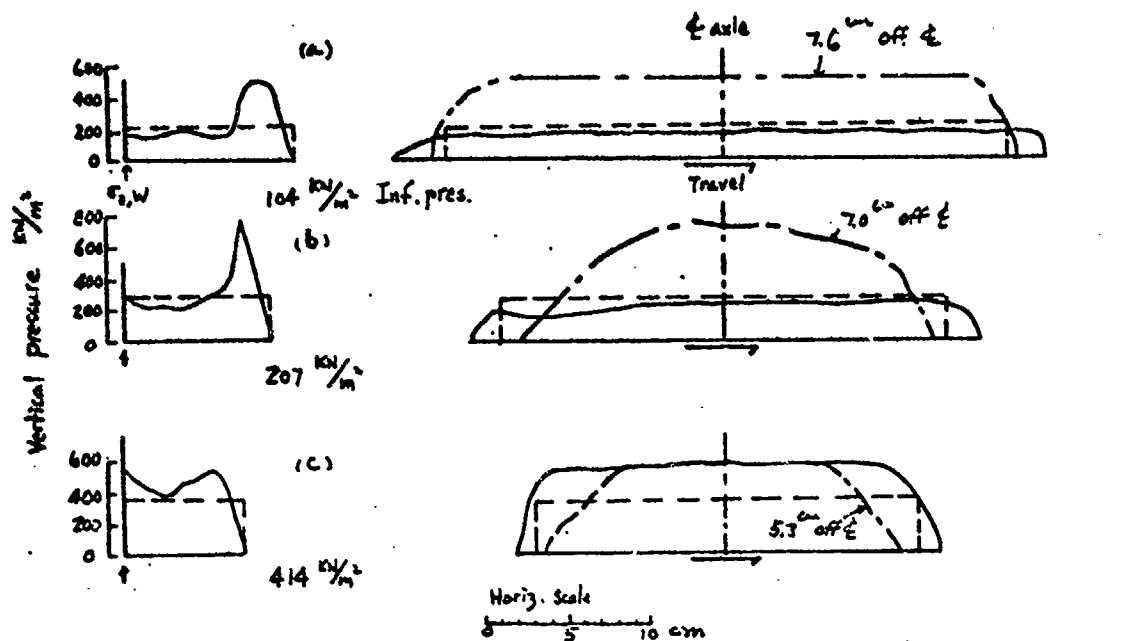


11.00-20, 12-PR Smooth tire
 207 MW/ft² inf. pres.
 6570-N Towed over clay
 wheel rolling at ~0.3 mps
 Penet. resist. 0-15 cm = 303 MW/ft²



Direction of travel

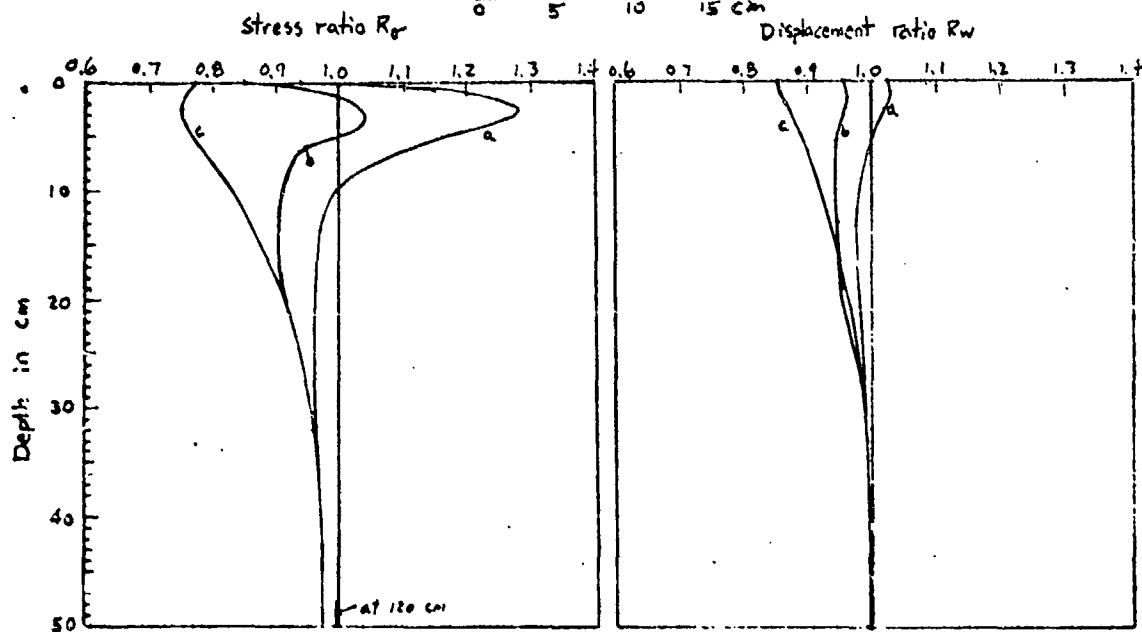
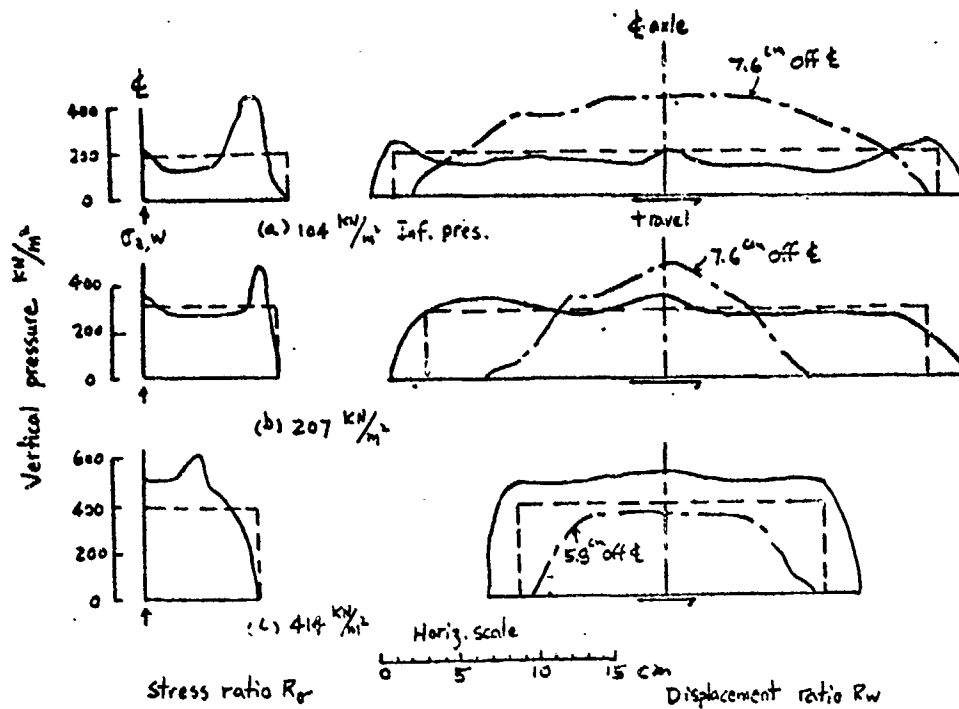
21.



- Measured pressure distribution along ξ
- - - Measured pressure distribution along offset line
- - - Uniformly distributed pressure

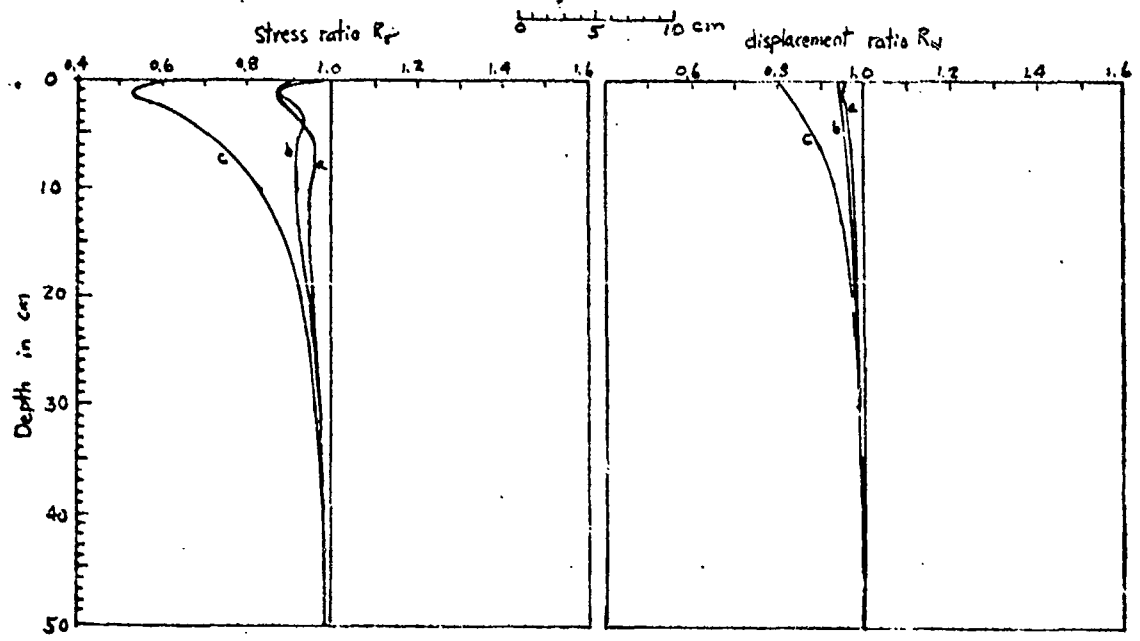
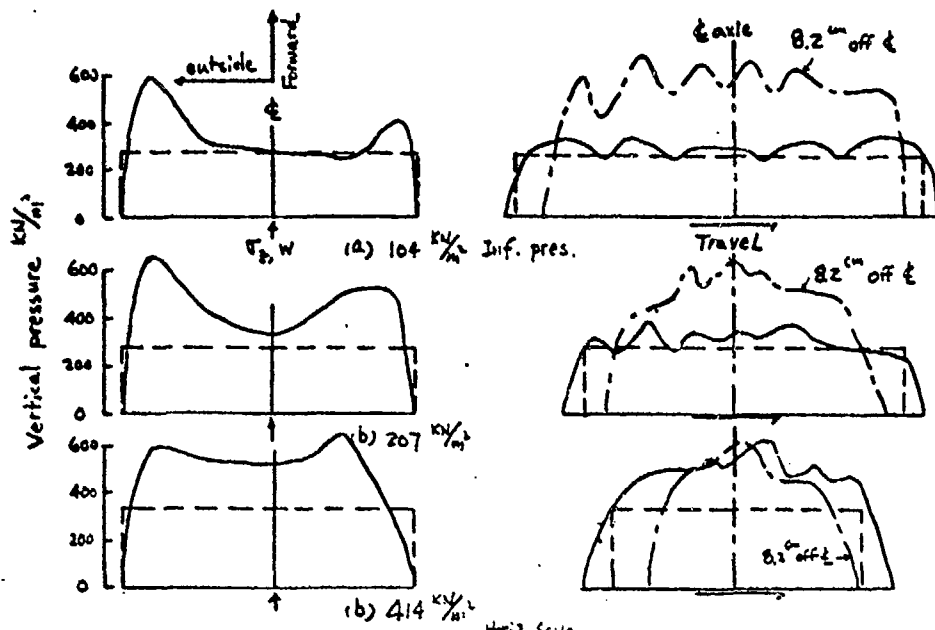
11.00-20, 12-PR smooth tire
 13350-N Towed wheel on firm surface
 wheel rolling at ≈ 0.7 mps

PLATE 2



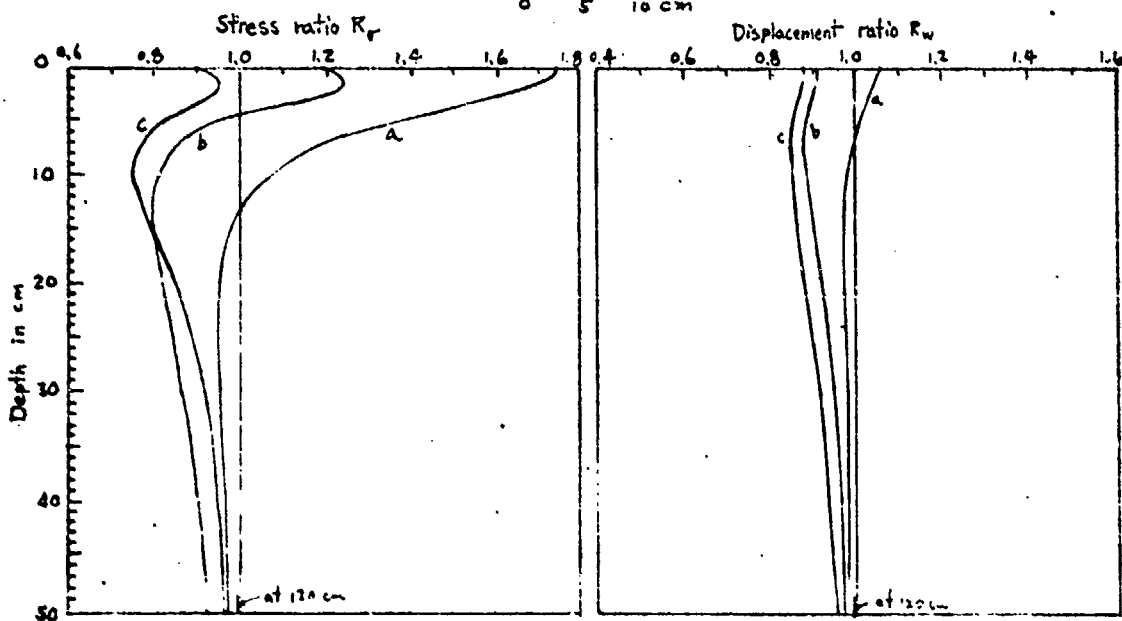
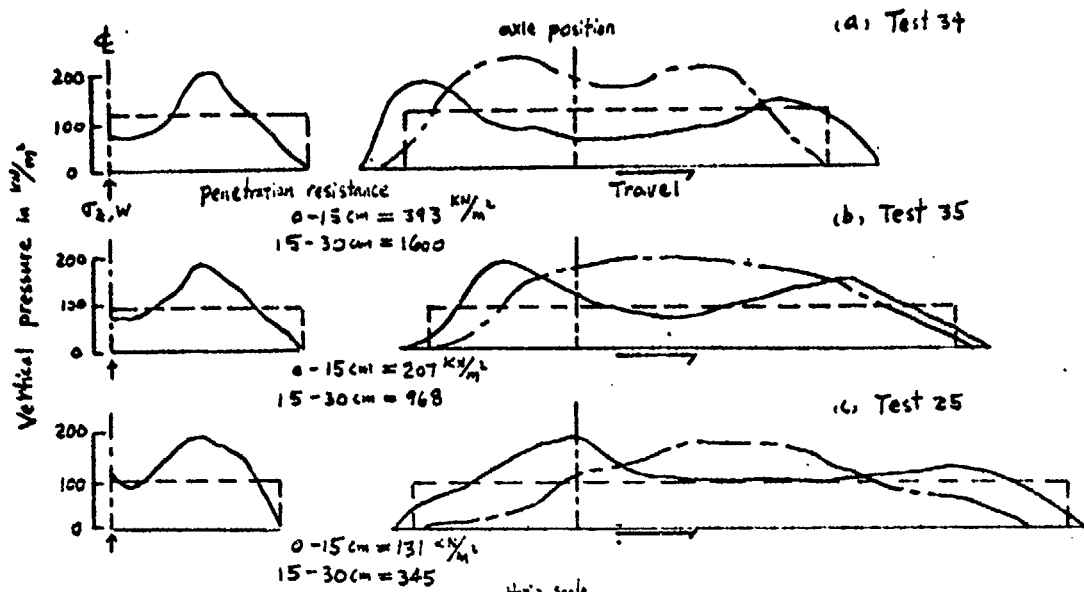
- Measured pressure distribution along ϵ
- - - Measured pressure distribution along offset line
- - - Uniformly distributed pressure

11.00-20, 12-PR smooth tire
 12,370-N static load
 on firm surface



- Measured pressure distribution along ξ
- - - Measured pressure distribution along offset line
- - - Uniformly distributed pressure

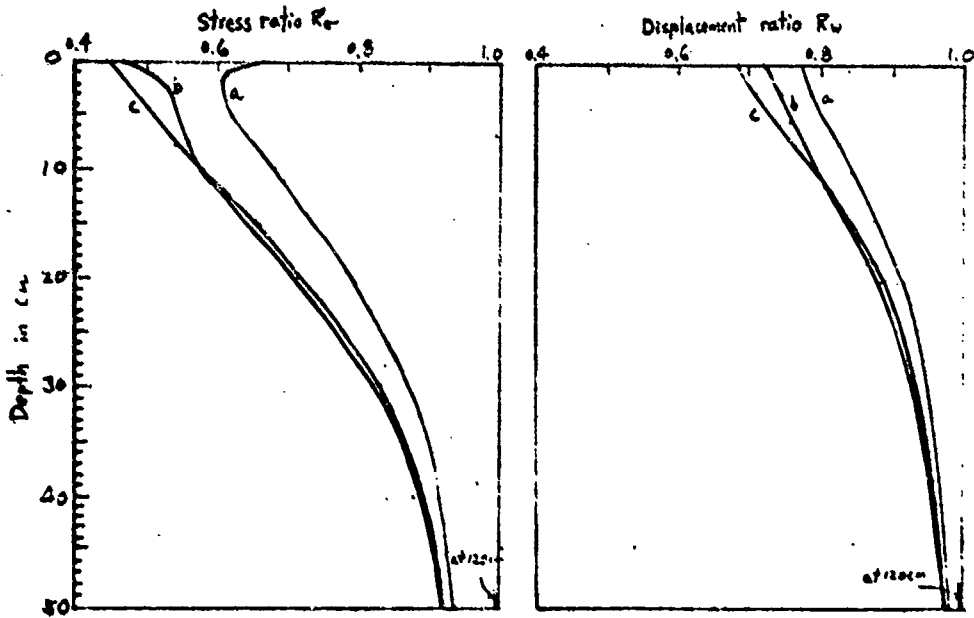
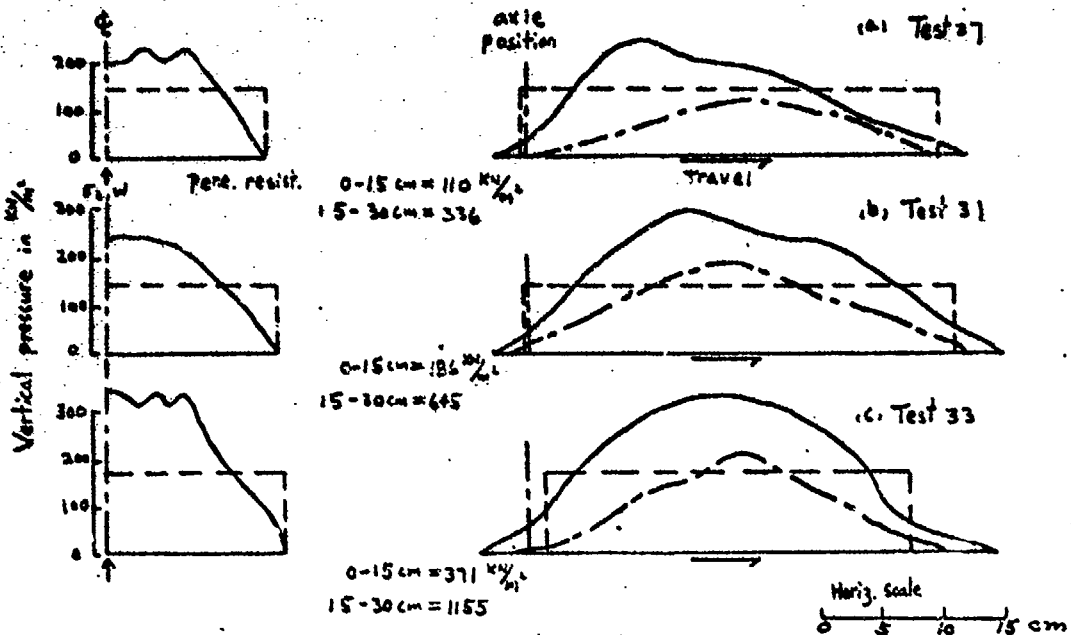
12-22.5, 12-PR tubeless tire
 12,450-N static load on firm surface



- Measured pressure distribution along ϕ
- - - Measured pressure distribution along 9.5 cm offset line
- - - Uniformly distributed pressure

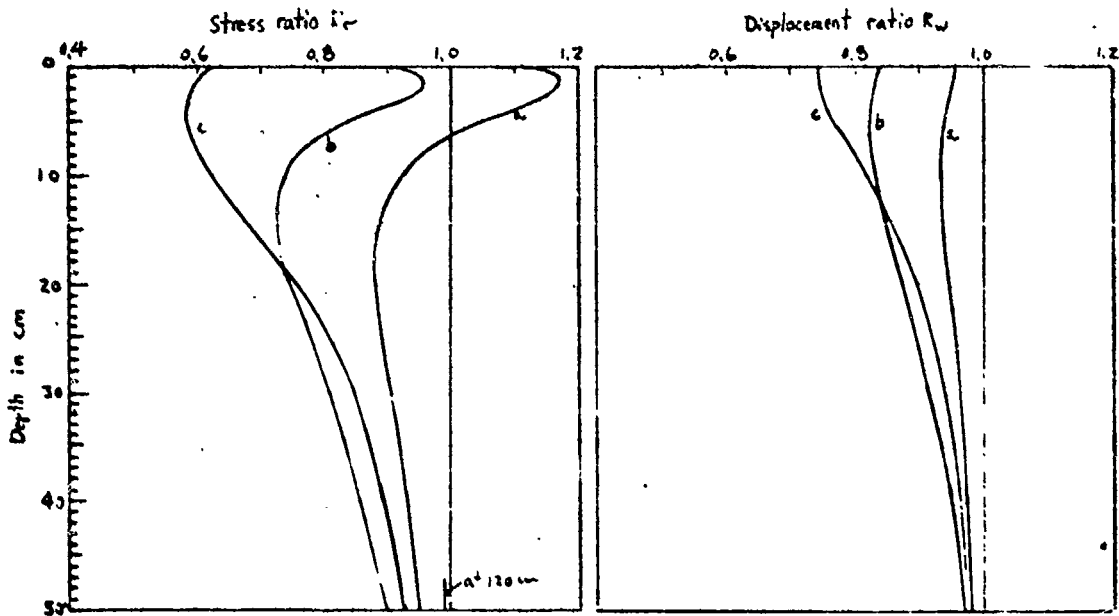
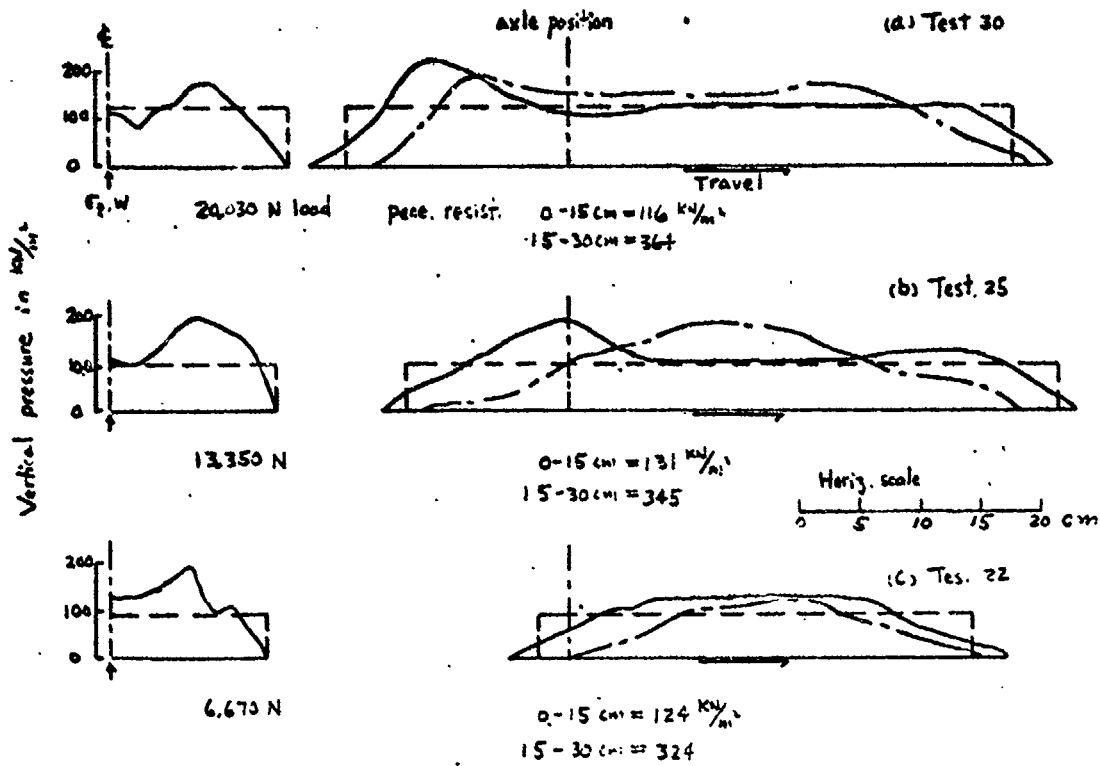
11.00-20, 12-PR smooth tire
 104 PSI inflation pressure
 13,350-N towed wheel on sand
 wheel rolling at ~ 0.8 mps

PLATE 5



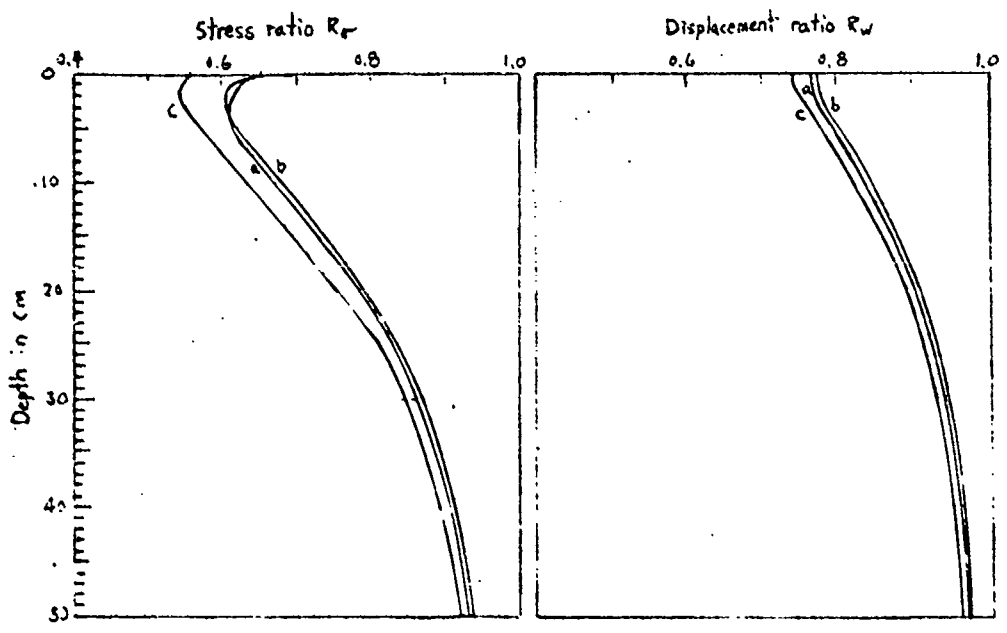
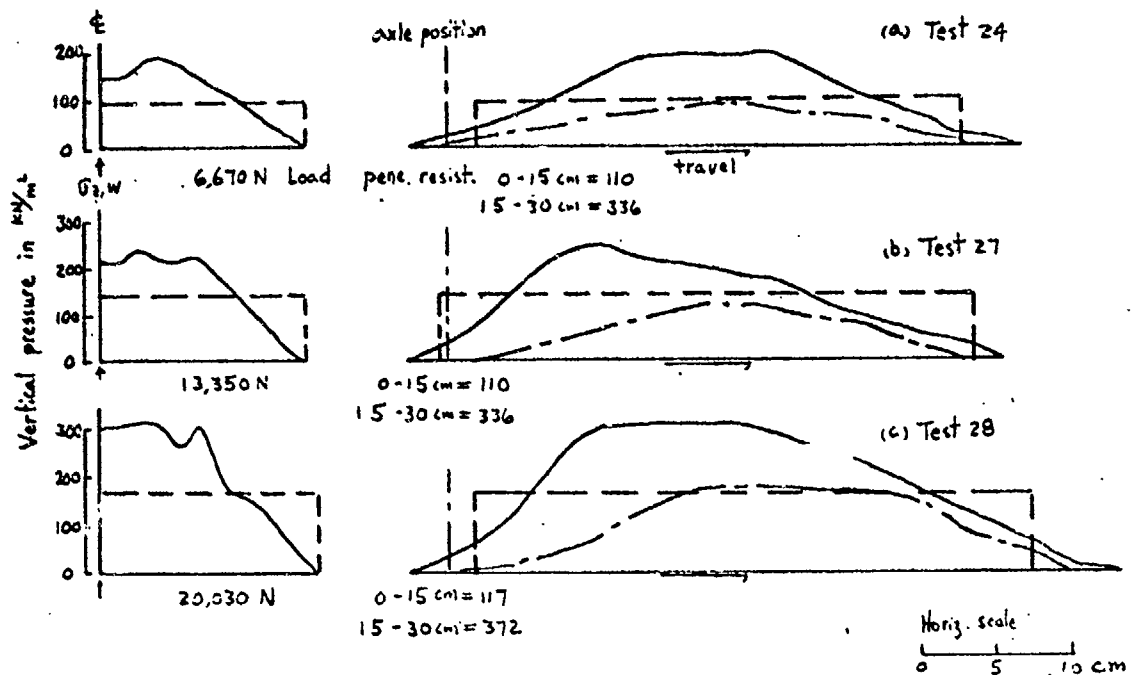
- Measured pressure distribution along ϕ
- - - Measured pressure distribution along 4.5 cm offset line
- - - Uniformly distributed pressure

11.00-20, 12-PR Smooth tire
 414 $\frac{KN}{m^2}$ inf. pressure
 13,350-N Towed wheel on sand
 wheel rolling at 0.8 mps



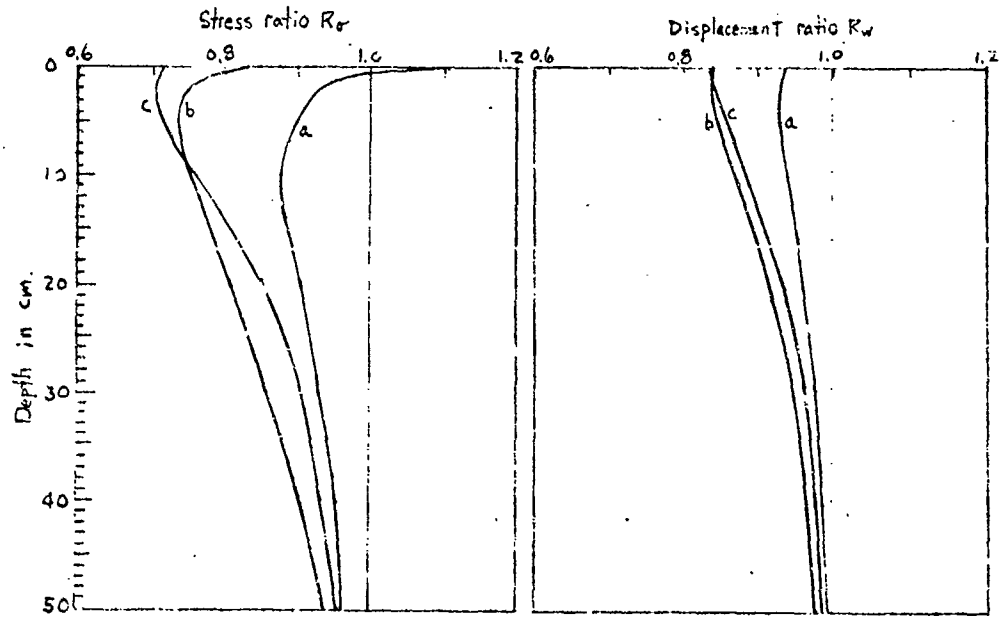
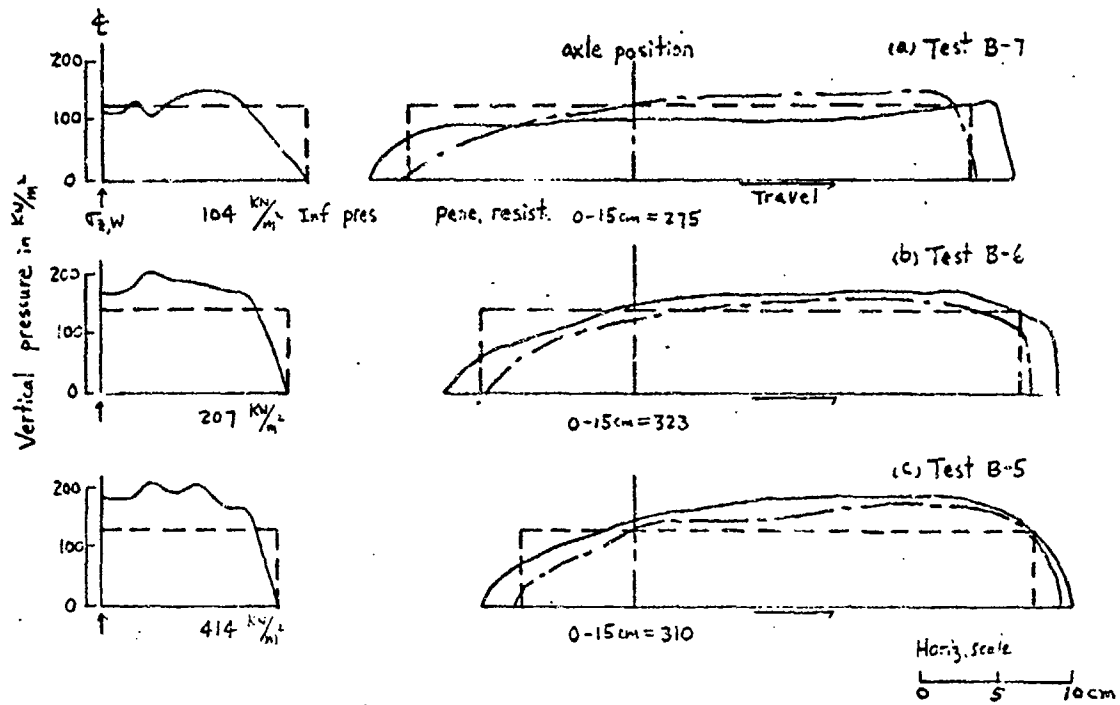
- Measured pressure distribution along ϵ
- - - Measured pressure distribution along 9.5° offset line
- - - Uniformly distributed pressure

11.00-20, 12-PR smooth tire
 109 kN/m^2 inf. pres.
 towed wheel on sand at ~ 0.3 mps



— Measured pressure distribution along ξ
 - - - Measured pressure distribution along 9.5° effort line
 - - - Uniformly distributed pressure

11.00-20, 12-PR smooth tire
 4.4 $\frac{\text{kg}}{\text{cm}^2}$ Inf. pres.
 towed wheel on sand at ≈ 0.3 mps

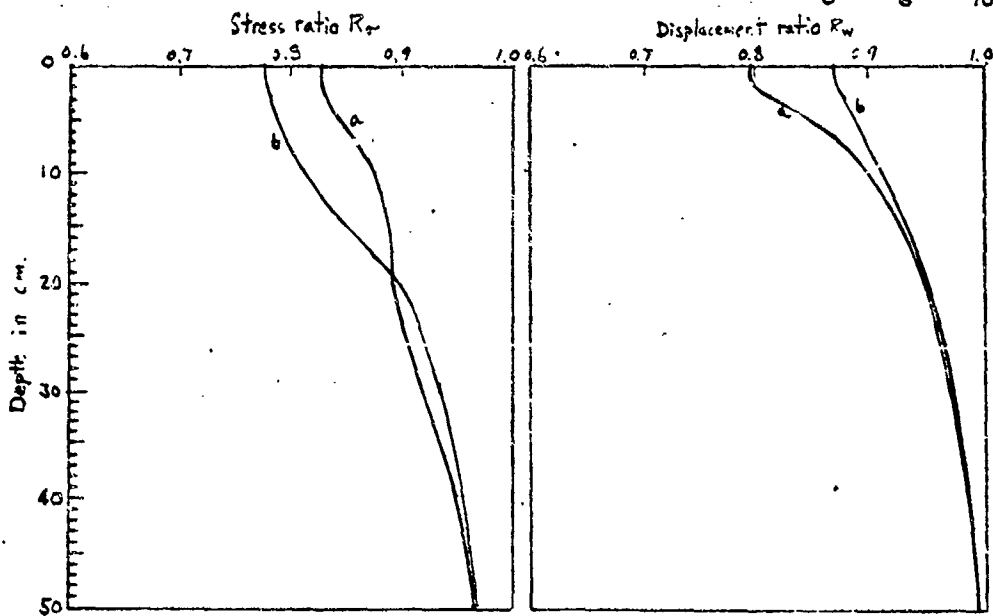
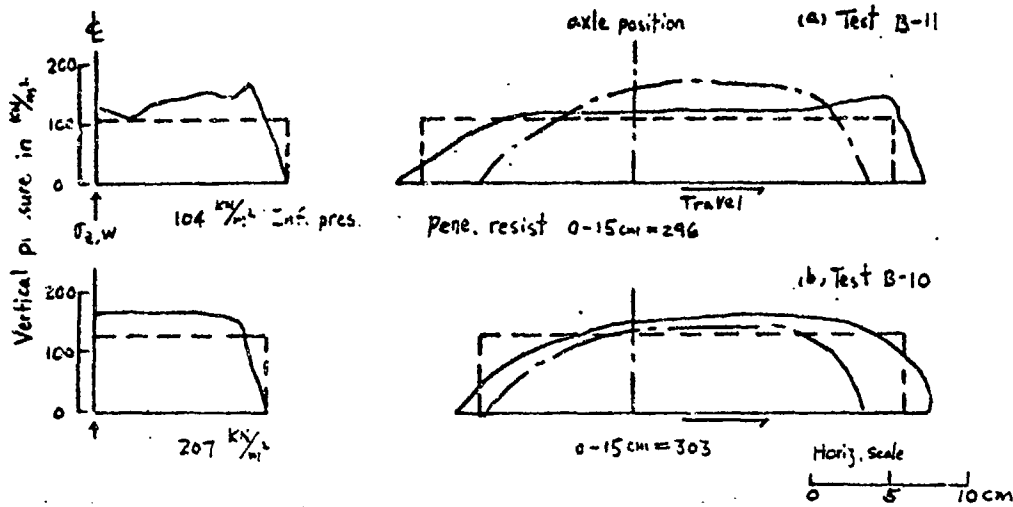


— Measured pressure distribution along ϕ

- - - Measured pressure distribution along 4.5" offset line

- - - Uniformly distributed pressure

11.00-20, 12-PR smooth tire
 13,350-N towed wheel on clay
 wheel rolling at ~ 0.3 mps



- Measured pressure distribution along ξ
- - - Measured pressure distribution along 9.5 cm offset line
- · · Uniformly distributed pressure

11.00-20, 12-PR smooth tire
 6.670-N towed wheel on clay
 wheel rolling at $\approx 3.3 \text{ m/s}$

Reproduced from
 best available copy.